

# Scaling relations for energy magnitudes

R. Das<sup>1\*</sup>, C. Meneses<sup>1</sup>

<sup>1</sup>) Catholic University of the North, Av. Angamos 0610, Antofagasta, Chile

Homogenizing earthquake catalogs is an effort critical to fundamentally improving seismic studies for next-generation seismology. The preparation of a homogenous earthquake catalog for a seismic region requires scaling relations to convert different magnitude types, like the  $m_b$  and  $M_s$ , to a homogenous magnitude, such as the seismic moment scale,  $M_{wg}$ , and energy magnitude scale,  $M_e$ . Several recent studies addressed the preparation of homogenized earthquake catalogs, usually involving the estimation of proxies of moment magnitude  $M_w$  from local,  $M_L$ , and teleseismic ( $M_s$  and  $m_b$ ) magnitude estimates. Instead of the standard least squares (SLR), most of such studies used the general orthogonal regression (GOR), while some used the Chi-square regression method. Here we critically discuss GOR and Chi-square regression theory and find that both are the same for the linear case — as expected since both stem from the same mathematical concept. Thus to foster an improved understanding of seismicity and seismic hazard, we used GOR methodology and derived global scaling relations individually between body, surface, energy, and seismic moment magnitude scales. For that purpose, we have compiled 13,576 and 13,282 events for  $M_s$  from ISC and NEIC, respectively,  $m_b$  magnitude data for 1,266 events from ISC, 614 events from NEIC, and  $M_{wg}$  magnitude values for 6,690 events from NEIC and GCMT. We have also derived  $M_{s,ISC}$ -to- $M_e$  and  $M_{s,NEIC}$ -to- $M_e$  conversion relations in magnitude ranges of  $4.7 \leq M_{s,ISC} \leq 8.0$  and  $4.5 \leq M_{s,NEIC} \leq 8.0$ , respectively. Likewise, we obtained  $m_{b,ISC}$ -to- $M_e$  and  $m_{b,NEIC}$ -to- $M_e$  conversion relations for ranges of  $5.2 \leq m_{b,ISC} \leq 6.2$  and  $5.3 \leq m_{b,NEIC} \leq 6.5$ . Since the number of data points was insufficient to derive the relations, we considered  $m_{b,NEIC}$  up to  $M6.5$ . Finally, we derived an  $M_{wg}$ -to- $M_e$  conversion relation for the  $5.2 \leq M_w \leq 8.2$  range of magnitudes with focal depths  $< 70$  km. Our scaling relations can be used for homogenizing earthquake catalogs and conducting seismicity and seismic hazard assessment studies with enhanced realism.

*Key words*—energy magnitude scale, Das Magnitude Scale (DMS), seismic moment magnitude scale, orthogonal regression.

## 1. INTRODUCTION

Earthquake magnitude is one of the descriptors most commonly used for earthquake size. Magnitude determinations for different earthquake occurrences in space and time generally lack consistency due to a complex inherent nature of the earthquake phenomenon and the use of different wave types and characteristics of recording instruments used for estimating earthquake size. The scaling relations between different magnitude scales (i.e.,  $m_b$ ,  $M_s$ ,  $M_w$ ,  $M_{wg}$ ,  $M_e$ ) are, therefore, of paramount importance for the homogenization of various magnitude scales into a preferred magnitude. A brief overview of different magnitude scales in use follows below.

Richter (1935) developed the local magnitude scale,  $M_L$ , first used only in a particular study area in California based on records obtained by a network of Wood Anderson seismometers. Reframing of his work has resulted in magnitude scales of various types, such as  $m_b$ ,  $M_s$ ,  $M_w$ ,  $M_e$ , and  $M_{wg}$ .

Gutenberg (1945a, b) was the first to introduce the body wave magnitude scale,  $m_b$ , which subsequently was reframed by Gutenberg and Richter (1956) based on the amplitude at distant stations. At present, ISC and NEIC (bulletins) consider the body wave magnitude the most complete. To measure earthquake si-

ze, one calculates the earthquake magnitude from the amplitude of the initial P-wave; to calculate an  $m_b$ , one uses the first few cycles of the short-period P waves recorded by short-period instruments. The ratio of maximum amplitude-to-period of P waves, with a period up to about 3 s, is used to determine the original Gutenberg body-wave magnitude (IASPEI, 2013):

$$m_b = \log_{10} \left( \frac{A}{T} \right) + Q(\Delta, h) - 3.0, \quad (1)$$

where  $A$  is P-wave ground amplitude in nm calculated from the maximum trace-amplitude in the first few P-wave cycles,  $T$  is period in seconds ( $T < 3$  s of the maximum P-wave trace amplitude),  $Q(\Delta, h)$  is attenuation function for PZ (P-waves recorded on vertical component seismographs) established by Gutenberg and Richter (1956) in the tabulated or algorithmic form, as used by the U.S. Geological Survey/National Earthquake Information Center (USGS/NEIC),  $\Delta$  is epicentral distance in degrees ( $20^\circ \leq \Delta \leq 100$ ), and  $h$  is focal depth in km.

\* Correspondence to: [ranjit.das@ucn.cl](mailto:ranjit.das@ucn.cl), [ranjit244614@gmail.com](mailto:ranjit244614@gmail.com).

The surface wave magnitude  $M_s$  is determined by NEIC, using the vertical component of Rayleigh waves with the 18–22 s periods recorded at different epicentral distances, whereas ISC uses both the vertical and horizontal components for 10–60 s periods (Petrova and Gabsatarova, 2019). The formula for determining surface wave magnitude is (Vanek et al., 1962):

$$M_s = \log_{10} \left( \frac{A}{T} \right)_{\max} + 1.66 \log \Delta + 3.3, \quad (2)$$

where  $A$  is the maximum horizontal component of any period and  $\Delta$  is the epicentral distance in km.

The magnitude scales discussed in the above behave non-uniformly, e.g., the  $M_L$ ,  $m_b$ , and  $M_s$  all have different saturation thresholds for larger-magnitude earthquakes, which can give rise to underestimation or overestimations of the actual ground motions. Since this poses a limitation on the measurement using these magnitude scales, the need to overcome these limitations became a priority. To address this problem, Hanks and Kanamori (1979) proposed a magnitude scale called moment magnitude,  $M_w$ , defined as:

$$M_w = \frac{2}{3} \log M_o - 10.7, \quad (3)$$

where  $M_o$  is the seismic moment in dyne-cm. The formulation of the  $M_w$  scale, Eqn. (3), is based mainly on Southern California seismicity, and the terms in the  $M_w$  scale, Eqn. (3), are the result of substitution. The  $(2/3 \log M_o - 10.7)$  scale is achieved by substituting the ratio of energy ( $E$ ) and seismic moment  $M_o$ , i.e., as  $E/M_o = (\Delta\sigma) / 2\mu = 5 \times 10^{-5}$ , where  $\sigma$  is earthquake stress drop, and  $\mu$  is the shear modulus in the Gutenberg-Richter energy magnitude equation  $\log E = 1.5 M_s + 11.8$ . Therefore, the  $M_w$  scale is formulated based on substitution rather than a directly observed seismic moment. Moreover, the  $M_w$  scale is not matched well at the global level with other magnitude scales, e.g., the  $m_b$  or  $M_s$ . Das et al. (2019) have developed an advanced seismic moment magnitude scale, called *Das magnitude scale* and denoted by  $M_{wg}$ :

$$M_{wg} = \frac{\log M_o}{1.36} - 12.68. \quad (4)$$

The superiority of the  $M_{wg}$  scale over the  $M_w$  is primarily due to four reasons:

(a) The  $M_w$  scale underestimates the largest earthquakes such as Tohoku-Oki of March 11, 2011, and Sumatra of December 26, 2004, whereas the  $M_{wg}$  scale does not (Giacomo, 2011; Das et al., 2019; Bormann and Saul, 2009; Bormann 2020);

(b) Because the  $M_w$  scale is derived based on long-period surface wave magnitudes, it is not a good estimator for high-frequency or strong-motion amplitudes measurements useful in estimating potential shake damage of present earthquakes. On the other hand, the  $M_{wg}$  scale used the first few cycles of P-waves from 25,708 global events. Therefore, it is expected for the  $M_{wg}$  to be closely related to high-frequency ground motion. Further-

more, the  $M_{wg}$  scale is derived based on the  $M_o$  so that the  $M_{wg}$  (i.e.,  $\log M_o/1.36 - 12.68$ ) is formulated based on the relation between body-wave magnitude and  $M_o$ . Therefore, it is expected for the  $M_{wg}$  to relate more closely to both the low- and high-frequency spectra of a seismic signal (Das et al., 2019);

(c) The formulation of the  $M_{wg}$  scale is based on direct instrumentally measured observed  $M_o$ . On the other hand, the formulation of the  $M_w$  scale (i.e.,  $2/3 \log M_o - 10.7$ ) was based not on instrumentally measured observed  $M_o$  since the formula for  $M_w$  in terms of  $M_o$  was obtained using the following substitution:  $E/M_o = (\Delta\sigma) / 2\mu = 5 \times 10^{-5}$ , where  $\sigma$  is earthquake stress drop and  $\mu$  is the shear modulus in the Gutenberg-Richter energy magnitude equation  $\log E = 1.5 M_s + 11.8$ ;

(d) The  $M_{wg}$  scale considers proper representations of global seismicity in terms of small-, intermediate-, and high-magnitude events. On the other hand, the  $M_w$  scale is based primarily on the Southern California seismicity (specifically, small and intermediate events). The  $M_w$  scale overestimates radiated seismic energy and produces an error of 0.368 magnitude unit (m.u.) (Das et al., 2019).

The  $M_{wg}$  scale does not saturate for large earthquakes. Hence, it is directly proportional to the logarithm of  $M_o$ .  $M_o$  is a direct indicator of the parameters related to earthquake source mechanisms like fault area, slip, and rigidity. Therefore, it provides a truthful representation of the actual ground motions for all magnitude ranges. Hence the  $M_{wg}$  is preferably treated as a reliable scale for measuring the size of earthquakes, showing its strength for the compilation of earthquake catalogs with all magnitude ranges expressed in this unified  $M_{wg}$ , which, in turn, is used for seismic hazard estimation and other related seismological applications.

Another magnitude called energy magnitude, and denoted  $M_e$ , was developed by Choy and Boatwright (1995):

$$M_e = \frac{2}{3} \log E_s - 2.9, \quad (5)$$

where  $E_s$  denotes the seismic radiated energy. The  $M_{wg}$  and  $M_e$  are more suitable for estimating the seismic hazard assessment than any other scales. In general, applications of  $M_o$  range from shaking maps, seismic hazard maps to many other seismological uses. To better understand the seismicity and seismic hazard,  $M_e$  could be used together with the  $M_{wg}$  (Boatwright and Choy, 1986; Choy and Kirby, 2004) for preparing a homogeneous earthquake catalog.

The preparation of a homogeneous earthquake catalog for a seismic region requires scaling relations between different magnitudes and a preferred one. However, catalogs containing seismic moments from either  $M_L$ ,  $m_b$ , or  $M_s$  magnitudes - or direct measurements - already exist. Various studies, e.g., by Yadav et al. (2009) and Bormann and Giacomo (2010), suggest that seismic hazard assessment and seismicity studies using energy magnitude are an added advantage. Indeed, due to the complexities of the determination,  $M_e$  magnitudes are not widely available. Therefore, scaling (or regression) relations between various magnitude types - such as  $m_b$ ,  $M_s$ ,  $M_{wg}$ , and  $M_e$  - would enable the preparation of a catalog in terms of  $M_e$  for a better understanding of seismicity via energy.

The regression methodologies used for such scaling relations, therefore, should be free from any bias introduced during the conversion of magnitudes since every bias in magnitude conversion leads to erroneous results in the parameters of Gutenberg Richter frequency-magnitude distribution as well as in seismic hazard estimation (Castellaro et al., 2006; Das et al., 2018). Scaling relations are usually based on Standard Linear Regression (SLR) procedures, but SLR is valid only when one of the variables contains errors, whereas, in magnitude conversion problems, both the dependent and independent variables have errors. So, the use of the SLR procedure will lead to incorrect estimates. In such situations, it is appropriate to use the GOR regression procedure for magnitude conversions only (Das et al., 2012, 2013, 2014, 2018; Thingbaijam et al., 2008; Ristau, 2009). However, GOR has a significant overestimation problem, as reported by Carroll and Ruppert (1996) and other researchers (e.g., Stefanski, 2000; Carroll et al., 2006; Das et al., 2018). To reduce the overestimation problem, Das et al. (2018) have recently developed a new GOR method - in which bias is handled well through an intermediate step.

One of this study's objectives is to provide a detailed overview of the regression procedures (mainly General Orthogonal Regression) and their applications for developing scaling relations for the conversions of  $m_b$ ,  $M_s$  and  $M_{wg}$  into  $M_e$ . The  $M_e$  sparseness is alleviated using such conversion relations to understand the seismicity and seismic hazard assessment of a region.

## 2. METHODOLOGY FOR REGRESSION RELATION

### 2.1. Standard Least-Squares Regression (SLR)

The most common and simplest regression method used in statistical applications is the Standard Least-Squares Regression (SLR). SLR encompasses minimizing the squares of the vertical residuals to the best fitting line. However, SLR is not appropriate when both regression variables contain an error.

### 2.2. General Orthogonal Regression (GOR)

The General Orthogonal Regression (GOR) method has long been of interest for researchers in different areas since Adcock (1878). Early studies focused on GOR derivation, often in different ways. The contributors included Adcock (1878), Kummel (1879), Pearson (1901), Lindley (1947), Madansky (1959), and many others. GOR method was discovered and rediscovered many times by various researchers (e.g., Anderson, 1984; Carroll and Rupert, 1996; Das et al., 2012; Wason et al., 2012; Das et al., 2014; Das et al., 2018). The goal of GOR is to account for the effects of measurement errors in both variables. GOR occurs when (1) two methods intend to measure the same quantity, or (2) when two variables are related to each other by following the same physical laws (Carroll and Rupert, 1996). The GOR procedure minimizes the statistical Euclidean distance between given points and their corresponding theoretical (statistically true) points along the GOR line. The basics of the GOR procedure are discussed in the literature, e.g., by Madansky (1959), Kendall and Stuart (1979), Fuller (1987), Carroll and Ruppert (1996), Das et al. (2011, 2013).

For observed data pairs  $(X_t, Y_t)$  with both elements having non-negligible measurement errors, a GOR relation is expressed as:

$$y_t = \beta_0 + \beta_1 x_t, \quad (6)$$

where  $x_t$  is the abscissa of the point on the GOR line, which is the statistical Euclidean projection of the given point  $(X_t, Y_t)$ , and  $\beta_0$  and  $\beta_1$  represent the slope and the line's intercept, respectively. Different researchers commonly use the above GOR relation, Eqn. (6), by replacing  $x_t$  with  $X_t$ , as follows:

$$y'_t = \beta_0 + \beta_1 X_t, \quad (7)$$

The estimate  $y'_t$  in Eqn. (7) differs from the actual estimate  $y_t$  in the GOR relation, Eqn. (6), as abscissa of the projected point on the GOR line,  $x_t$ , differs from abscissa of the given point,  $X_t$ . This incorrect form of GOR, Eqn. (7), produces a serious mathematical and conceptual blunder. This GOR form, Eqn. (7), is referred to as the conventional GOR or just GOR2 (Das et al., 2018). The incorrect GOR form results in an overestimated slope (Carroll and Ruppert, 1996; Carroll et al., 2006; Das et al., 2018). Carroll and Rupert (1996) stated that GOR2 overestimates the slope due to incorrect application, arguing that orthogonal regression often is misused in errors-in-variables linear regression because of a failure to account for equation errors; a typical result is to overcorrect for measurement error, that is, to overestimate the slope because equation error gets ignored. To correct the biases of GOR2, Carroll and Rupert (1996) have modified the method of estimating the error variance ratio's  $\eta$  value by adding equation error. Note that the use of different  $\eta$  values results in various lines for the same data pairs. Stefanski (2000) also addressed the bias of GOR2 - as a measurement error; see his section 2.1, 2<sup>nd</sup> para. p.1354). Recently, Das et al. (2018) suggested an algorithm for reducing GOR2 biases, referred to as GOR1.

The slope and intercept of the GOR line is given by

$$\hat{\beta}_1 = \frac{S_Y^2 - \eta S_X^2 + \sqrt{(S_Y^2 - \eta S_X^2)^2 + 4\eta S_{XY}^2}}{2S_{XY}} \quad (8)$$

and

$$\hat{\beta}_0 = \bar{Y}_t - \hat{\beta}_1 \bar{X}_t, \quad (9)$$

where  $S_Y^2$ ,  $S_X^2$ , and  $S_{XY}^2$  represent the sample covariance of  $Y_t$ ,  $X_t$ , and between  $Y_t$  and  $X_t$ , respectively;  $\bar{X}_t$ ,  $\bar{Y}_t$  are mean values of the independent and dependent variables, respectively. Here  $\eta$  denotes the error variance ratio value and is determined from the standard deviations of the dependent and independent variables, i.e.,  $\eta = \frac{\sigma_x}{\sigma_y}$ .

Let us assume  $\sigma_{uu}$ ,  $\sigma_{ee}$ ,  $\sigma_{eu}$ , and  $\sigma_{vv}$  to be the variances of  $X_t$ ,  $Y_t$ , between  $Y_t$  and  $X_t$ , respectively. The estimator  $\hat{\beta}_1$  is obtained by minimizing the statistical Euclidean distance (Fuller, 1987, Eqn. 1.3.20):

$$S_F = \frac{\sum_{t=1}^n (Y_t - \beta_0 - \beta_1 X_t)^2}{\sigma_{ee} - 2\beta_1 \sigma_{eu} + \beta_1^2 \sigma_{uu}} \quad (10)$$

GOR studies have continued based on the merits and demerits of the procedure considered. Since, in the development of a GOR relation, statistical Euclidean distance residuals are used, unbiased estimation of the dependent variable also requires considering the same statistical Euclidean distance criteria (Das et al., 2012; Wason et al., 2012; Das et al., 2014; Das et al., 2018). Statistical and seismological literature uses different terminology for denoting the statistical Euclidean distance. For example, Carroll and Ruppert (1996) use total ‘Euclidean distance’ or ‘orthogonal distance’ for  $\eta = 1$ , and ‘weighted orthogonal distance’ for denoting statistical Euclidean distance with  $\eta \neq 1$ . The issue of statistical Euclidean distance is explained below with the following two cases (Das et al., 2018).

**Case I:** — Consider an SLR line obtained using three data pairs  $(X_1, Y_1)$ ,  $(X_2, Y_2)$ , and  $(X_3, Y_3)$ , with their corresponding theoretical true points on the SLR line being  $(x_1, y_1)$ ,  $(x_2, y_2)$ , and  $(x_3, y_3)$ , respectively. These points on the line are used to derive the best-fitting SLR line by minimizing the vertical residuals. On substituting  $X_1$ ,  $X_2$ , and  $X_3$  in the obtained SLR line, the theoretical true points  $((x_1, y_1)$ ,  $(x_2, y_2)$ , and  $(x_3, y_3)$ ) used in the derivation of the best fitting SLR line (Fig. 1a) can be obtained. These Euclidean distances are used during the development of the SLR line.

**Case II:** — A GOR line is developed using observed data pairs  $(X_1, Y_1)$ ,  $(X_2, Y_2)$ , and  $(X_3, Y_3)$  - with errors in both variables. The theoretical true points of these data pairs are on the GOR line, i.e.,  $(x_1, y_1)$ ,  $(x_2, y_2)$ , and  $(x_3, y_3)$  are obtained by minimizing the Euclidean distance (statistical Euclidean distance or weighted orthogonal distance). Unlike in case I, substituting  $X_1$ ,  $X_2$ , and  $X_3$  in the GOR line, Eqn. (6), does not result in the corresponding theoretical true points. Instead of obtaining theoretical true points, different points altogether are obtained on the GOR lines, Fig. 1b. Therefore, GOR2 introduces a bias in the estimation, as it is not possible to get a corresponding true point via direct substitution of any observed value of the independent variable on the GOR line.

Solutions for reducing the GOR overestimation problem have been proposed, namely by Wason et al. (2012), Das et al. (2012), (2013), (2014), and (2018).

Recently, Das et al. (2018) suggested a simple procedure to reduce the GOR overestimation problem. Below given is a brief description of Das et al. (2018):

(a) For deriving the GOR relation, an observed dataset of events with  $X_t$ ,  $Y_t$  values must be considered. With this dataset given, the development of a GOR relation is necessary.

(b) For each observed data pair  $(X_t, Y_t)$ , the corresponding (statistically) true theoretical point  $(x_t, y_t)$  on the GOR line is obtained via statistical Euclidean distance on the derived GOR line from point  $(X_t, Y_t)$ .

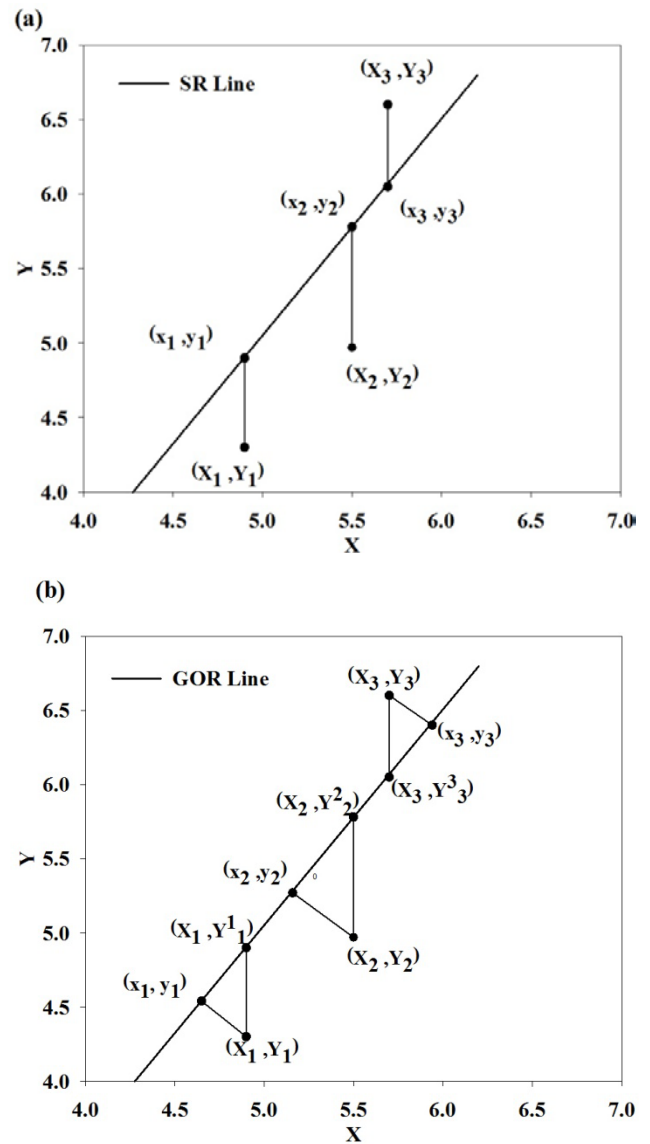


Figure 1. Regression plots showing the theoretical true points  $(x_t, y_t)$  and the corresponding (given) observed value  $(X_t, Y_t)$  using (a) SLR and (b) GOR. Plots also show the deviations (in the case of SLR, e.g.,  $y_t - y_1$ , and in the case of GOR  $y_t - Y_1$ ) between the theoretical true values  $y_t$  and the estimated dependent variables on direct substitution of  $X_t$  in Eqn. (7). The plot in (b) also shows that the Euclidean distance used during GOR derivation does not remain the same as in the estimation (Das et al., 2018). The plots in (a) and (b) are a schematic representation for SLR and GOR, respectively. The locus of the two lines (SLR and GOR) is made the same for easiness to explain the GOR methodology. For most of the  $\eta$  values, the two lines (SLR and GOR) are not the same as depicted.

For the GOR relation,  $X_t$  value cannot be substituted directly on the right-hand side of the GOR relation obtained in step (a). This type of mathematical error is called a measurement error (Stefanski, 2000). This incorrect practice will provide an over-estimated slope, as reported by Carroll and Ruppert (1996) and Das et al. (2018).

Step (b) above does not apply to those events where only  $X_t$  is known, but  $Y_t$  value is unknown. In such cases, the determination of predicted  $Y_t$  for a given  $X_t$  requires the development of a linear relation between  $X_t$  and  $y_t$  values. This linear relation can be used to determine the  $y_t$  value corresponding to any given  $X_t$  value. The determined  $y_t$  value for a given  $X_t$  is not the physically true value; it is the best unbiased value. There is no

difference in the procedure of Das et al. (2018) that leads to the estimation of slope and intercept of the GOR lines from the approach followed by other investigators (e.g., Fuller, 1987). The difference between Das et al. (2018) and commonly used approaches is in estimating the theoretical true value of  $(x_i, y_i)$  corresponding to any observed value  $(X_i, Y_i)$ . For correction of GOR2 biases, Carroll and Rupert (1996) introduced equation error in the estimation of  $\eta$  value, whereas Das et al. (2018) corrected the errors via an intermediate step - using an SLR relation between  $y_i$  and  $X_i$ . Both methods - by Carroll and Rupert (1996) and by Das et al. (2018) - reduce biases of GOR2.

### 2.3. Chi-Square Regression

The Chi-Square Regression technique used in recent seismological literature stems from Stromeyer et al. (2004), according to whom the Chi-square equation is as follows:

$$S_{\text{chi-square}} = \frac{\sum_{i=1}^N (M_{Si} - am_{bi} - b)^2}{\sigma^2(M_{Si}) + a^2\sigma^2(m_{bi})} \quad (11)$$

In the above,  $M_{Si}$  and  $m_{bi}$  denote the surface wave and body wave magnitudes, respectively. In this study,  $M_{Si}$  and  $m_{bi}$  represent the dependent and independent variables, respectively. The terms 'a' and 'b' represent slope and intercept, respectively. The equation denominator is the approximation of  $\text{var}(M_{Si} - am_{bi} - b)$  from Gauss error propagation law (Press et al., 1992):

$$\begin{aligned} \text{var}(M_{Si} - am_{bi} - b) &\approx \\ &\approx \text{var}(M_{Si}) \left( \frac{\delta(M_{Si} - am_{bi} - b)}{\delta(M_{Si})} \right)^2 \\ &+ \text{var}(M_{bi}) \left( \frac{\delta(M_{Si} - am_{bi} - b)}{\delta(M_{bi})} \right)^2 = \\ &= \sigma^2(M_{Si}) + a^2\sigma^2(m_{bi}). \end{aligned} \quad (12)$$

GOR, as discussed by Fuller (1987), and Chi-square regression, Eqn. (11), as discussed by Stromeyer et al. (2004), are the same for the linear case. Both equations are the same except for the terminology  $2\beta_1\sigma_{eu}$ . Stromeyer et al. (2004) considered the case of uncorrelated errors between dependent and independent variables. In the case of uncorrelated error, the term  $\beta_1\sigma_{eu}$  becomes zero. Hence, GOR in the statistical literature (e.g., Fuller, 1987) and Chi-square regressions in the seismological literature are the same. Lolli and Gasperini (2012, p.1) stated that both GOR2 and Chi-square provide (CSQ) almost the same results and concluded that GOR2 and Chi-square methods are substantially equivalent. Lolli and Gasperini (2012) also claimed that computed coefficients coincide for Chi-square and GOR2 up to the fifth significant digit. We find both of these methods to be mathematically the same for linear cases. Therefore, slope, intercept, and their associated uncertainties will also be the same. Hence, there is hardly any advantage in using a different name (Chi-square Regression) instead of GOR; on the contrary, it creates some misgivings about the GOR procedure.

### 3. DATA

This study considers data from various sources worldwide, collected between 01 January 1976 and 31 May 2007. The data sources are International Seismological Center (ISC), U.K. (<http://www.isc.ac.uk/search/Bulletin>, last accessed in August 2010); National Earthquake Information Center (NEIC), the USGS, USA (dead link <http://neic.usgs.gov/neis/epic/epic-global.html>, last accessed in August 2010); and HRVD (since 1976, now operated as the Global Centroid-Moment-Tensor project at the Lamont Doherty Earth Observatory (LDEO) (<http://www.globalcmt.org/CMTsearch.html>, last accessed in October 2010) earthquake data bulletins.

We compiled in our study the body wave magnitude values for 1,266 events from ISC and 614 events from NEIC, and surface wave magnitude values for 13,576 events from ISC and 13,282 events from NEIC. Furthermore, we also compiled moment magnitude values for 6,690 events from GCMT and NEIC. Finally, we used energy magnitude values of 6,690 events by NEIC.

### 4. MAGNITUDE CONVERSION RELATIONS

To understand the correlations among magnitude scales and improve the understanding of seismicity and seismic hazard assessment, scaling relations amongst different magnitudes ( $m_b$ ,  $M_s$ ) and  $M_e$ , were developed. SLR, GOR1, and GOR2 procedures are used for that purpose, as suggested in the recent literature (Das et al., 2018). However, a GOR relation requires the value of  $\eta$ . Here, GOR relations were estimated assuming  $\eta = 1$ , as suggested in other studies (Ristau, 2009, Bormann et al., 2009). However, these studies do not explain the reason for using  $\eta = 1$ .

#### 4.1. Conversion of Surface Wave Magnitudes into $M_e$

The comparison between surface wave magnitudes  $M_{s,ISC}$  and  $M_{s,NEIC}$  was made in various earlier studies and found to be similar, e.g., by Das et al. (2011), Utsu (2002), Scordilis (2006), Das and Wason (2010). In this study, the equivalence was checked by deriving relations using a newly developed GOR (GOR1) procedure for the magnitude ranges  $4.7 \leq M_{s,ISC} \leq 8.0$  and  $4.5 \leq M_{s,NEIC} \leq 8.0$ . The derived GOR relations are:-

$$M_{S,NEIC} = 0.9979 M_{S,ISC} (\pm 0.000113) + 0.007854 (\pm 0.005671), \quad (13)$$

$$R_{xy} = 0.983865, \text{RMSO} = 0.085097, n = 12896,$$

where  $R_{xy}$  is the correlation coefficient, and RMSO is the standard deviation of orthogonal errors (Wason et al., 2012). The above GOR relations show that both  $M_{s,ISC}$  and  $M_{s,NEIC}$  can be treated as nearly equivalent to each other and can be considered a homogenous dataset. These relations are depicted in Figure 2a.

The GOR1 relation between  $M_{S,ISC}$  and  $M_e$  was developed using  $\eta=1$  and is given as (Figure 2b):

$$M_e = 0.934257 M_{S,ISC} (\pm 0.001019) + 0.496029 (\pm 0.061527),$$

$$4.7 \leq M_{S,ISC} \leq 8.0 \quad (14)$$

$$R_{xy} = 0.90, \text{RMSO} = 0.1839, n = 980, h < 70\text{km}.$$

For the conversion of  $M_{S,NEIC}$  into  $M_e$ , the derived GOR1 is:

$$M_e = 0.891634 M_{S,NEIC} (\pm 0.001157) + 0.731056 (\pm 0.069539),$$

$$4.5 \leq M_{S,NEIC} \leq 8.0 \quad (15)$$

$$R_{xy} = 0.91, \text{RMSO} = 0.167, n = 586, h < 70\text{km}, \eta = 1.$$

The plot of  $M_{S,NEIC}$  into  $M_e$  is given in Figure 2c.

As reported above and in earlier studies, e.g., Das et al. (2011),  $M_s$  data are combined to develop a GOR1 relation between  $M_s$  and  $M_e$ . That equation is given below, while the plot is in Figure 2d:

$$M_e = 0.918348 M_s (\pm 0.000768) + 0.584035 (\pm 0.046311),$$

$$4.5 \leq M_s \leq 8.0 \quad (16)$$

$$R_{xy} = 0.90, \text{RMSO} = 0.178, n = 1566, h < 70\text{km}, \eta = 1.$$

#### 4.2. Conversion of Body Wave Magnitudes into $M_e$

Several studies have revealed that  $m_{b,ISC}$  and  $m_{b,NEIC}$  events are not equivalent (Das et al., 2011; Nath and Thingbaijam, 2010). For the conversion of  $m_{b,ISC}$  into  $M_e$ , we used the magnitude range  $5.2 \leq m_{b,ISC} \leq 6.2$ , and  $m_{b,NEIC}$  into  $M_e$  the magnitude range  $5.3 \leq m_{b,NEIC} \leq 6.5$  with focal depths  $< 70$  km. Datasets of 1,266 and 641 events of  $m_{b,ISC}$  and  $m_{b,NEIC}$ , respectively, were used to derive the GOR1 relations. GOR1 relations for  $m_{b,NEIC}$  to  $M_e$  and  $m_{b,ISC}$  to  $M_e$  are:

$$M_e = 1.468087 m_{b,NEIC} (\pm 0.005344) - 2.59471 (\pm 0.313607),$$

$$5.3 \leq m_{b,NEIC} \leq 6.5 \quad (17)$$

$$R_{xy} = 0.55, \text{RMSO} = 0.351, n = 641.$$

and

$$M_e = 1.42165 m_{b,ISC} (\pm 0.003872) - 2.17872 (\pm 0.224583),$$

$$5.2 \leq m_{b,ISC} \leq 6.5 \quad (18)$$

$$R_{xy} = 0.52, \text{RMSO} = 0.3844, n = 1266.$$

The plots of the given regression relations are in Figure 2e & 2f.

#### 4.3. Regression Relation between $M_{wg,GCMT}$ and $M_{wg,NEIC}$

We next obtain our regression relation between  $M_{wg,GCMT}$  and  $M_{wg,NEIC}$  from 6,690 events in the  $4.4 \leq M_{wg,NEIC} \leq 8.2$  magnitude range, and occurring from 1976-2007. The empirical relation is:

$$M_{wg,GCMT} = 1.006688 M_{wg,NEIC} (\pm 0.000113) - 0.05706 (\pm 0.006529),$$

$$4.4 \leq M_{wg,NEIC} \leq 8.2 \quad (19)$$

$$R_{xy} = 0.99, \text{RMSO} = 0.050419, n = 6690.$$

The plot of the above regression relation is in Figure 2g. Several earlier studies, e.g., Scordillis et al. (2006), had observed that  $M_{wg,GCMT}$  and  $M_{wg,NEIC}$  are equivalent, based on a correlation between them. Eqn. (19) shows that  $M_{wg,GCMT}$  and  $M_{wg,NEIC}$  approximately are equivalent.

#### 4.4. Conversion of Moment Magnitude $M_{wg}$ into $M_e$

The GOR1 conversion relation is obtained for  $M_{wg}$  into  $M_e$  by using the 1,385 events of the magnitude range  $5.2 \leq M_{wg} \leq 8.2$  with focal depths  $< 70$  km, and given as

$$M_e = 1.045084 M_{wg} (\pm 0.000955) + 0.15727 (\pm 0.057168),$$

$$5.2 \leq M_{wg} \leq 8.2 \quad (20)$$

$$R_{xy} = 0.896554, \text{RMSO} = 0.185835, n = 1385.$$

The plot of the above regression relation is given in Figure 2h.

#### 4.5. Linearity Test for Scaling Relations

The magnitude scaling relations in most literature are linear, e.g., Hanks and Kanamori (1979), Choy and Boatwright (1995), Scordillis et al. (2006), Das et al. (2011). However, several non-linear relations are also available, e.g., Giacomo et al. (2015). Unfortunately, no justification is provided in favor of linear or nonlinear relations, as fittings are based only on naked-eye observations. Here, the linearity of the scaling relations is validated using the Fuller (1986) model.

Fuller (1987) checked his model linearity by plotting the residuals ( $V_i$ ) between  $Y_t$  and  $y_t$  versus  $xt$ , e.g., F1.2.3 on p.26 in Figure 1.2.1 by Fuller (1987). It is worth noting that the  $xt$  are the theoretical true values. Figure 1.2.1 by Fuller (1987) shows that the residuals between  $56 < x_t < 96$  are both positive and negative. Around 55% of data have residuals positive and negative, 18% of data with  $x_t \geq 96$  have only positive residual values, while 27% of data with  $x_t \leq 56$  have all residuals positive. Thus, for around 45% of data, neither positive nor negative residual values are available. Fuller performed a linear GOR fitting on the dataset and stated that the plot in Figure 1.2.1 by Fuller (1987) contains no apparent anomalies.



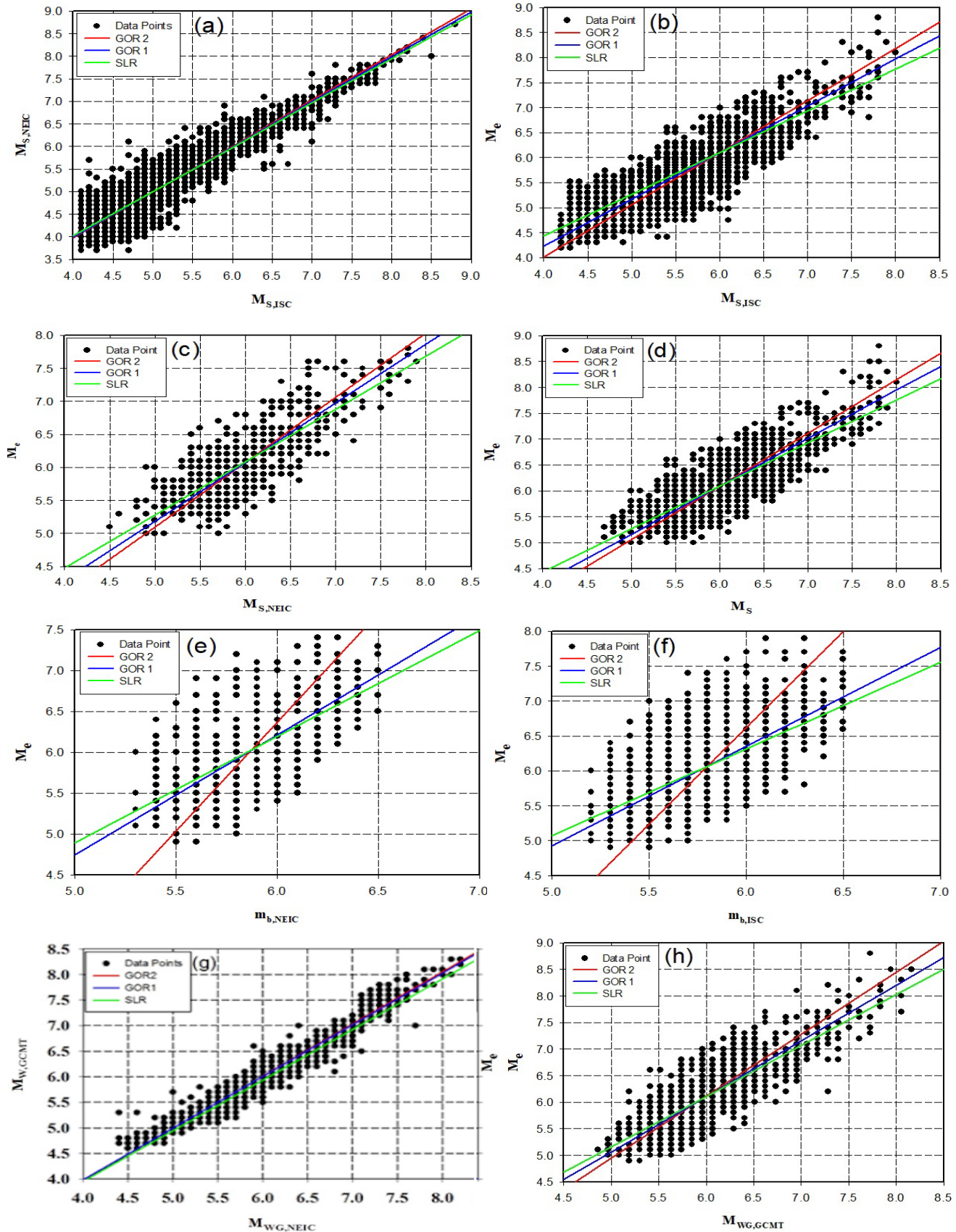


Figure 2. GOR1, GOR2, and SLR relations for different magnitudes: (a)  $M_{S,ISC}$  and  $M_{S,NEIC}$ , (b)  $M_{S,ISC}$  and  $M_e$ , (c)  $M_{S,NEIC}$  and  $M_e$ , (d)  $M_S$  and  $M_e$ , (e)  $m_{b,NEIC}$  and  $M_e$ , (f)  $m_{b,ISC}$  and  $M_e$ , (g)  $M_{WG,NEIC}$  and  $M_{WG,GCMT}$ , and (h)  $M_{WG}$  and  $M_e$  relation.

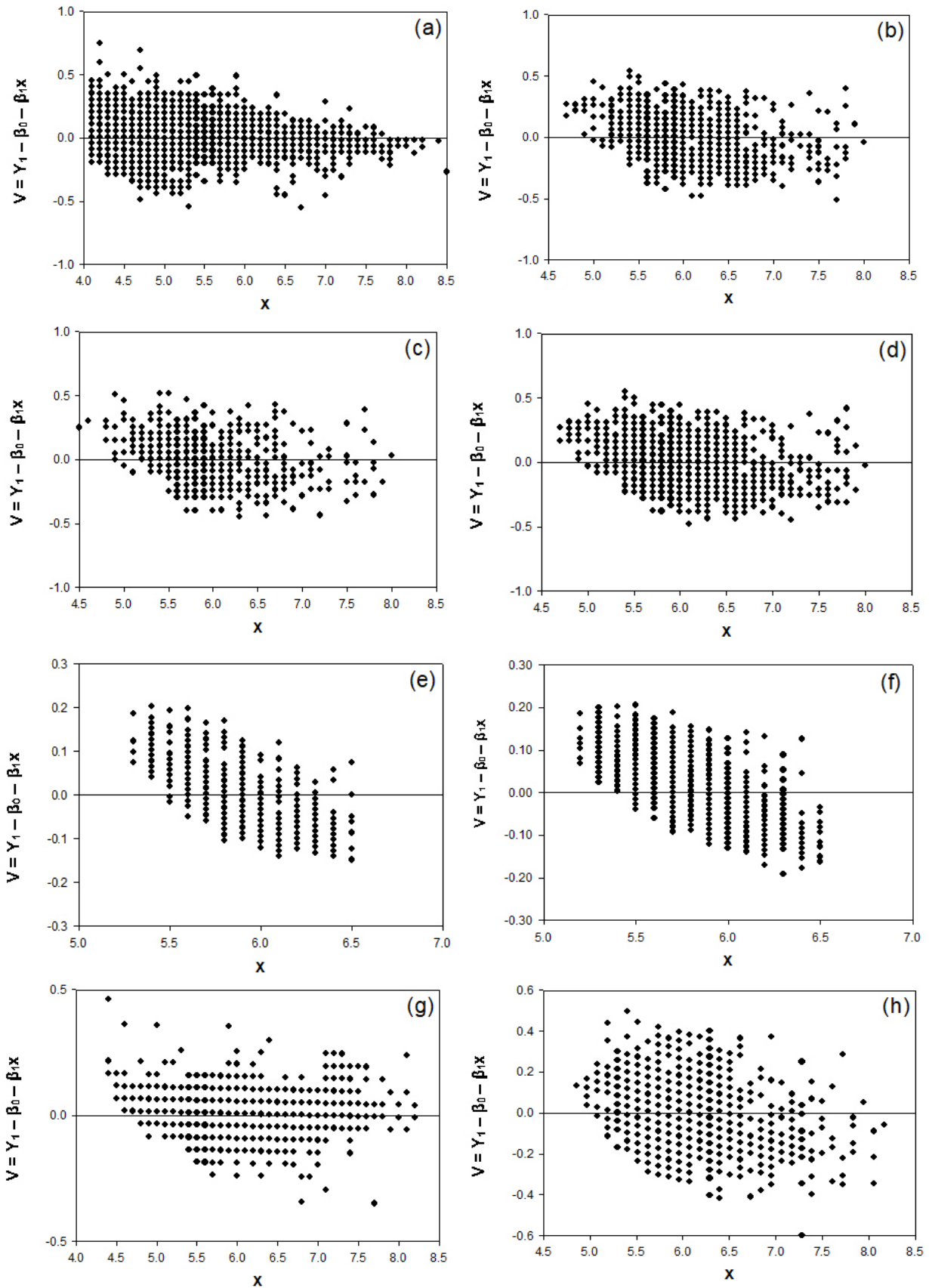


Figure 3. Residual plots using Fuller's (1986) statistical model for different magnitudes; (a)  $M_{S,ISC}$  and  $M_{S,NEIC}$ , (b)  $M_{S,ISC}$  and  $M_b$ , (c)  $M_{S,NEIC}$  and  $M_b$ , (d)  $M_s$  and  $M_b$ , (e)  $m_{b,ISC}$  and  $M_b$ , (f)  $m_{b,NEIC}$  and  $M_b$ , (g)  $M_{WG,NEIC}$  and  $M_{WG,GCMT}$ , and (h)  $M_{WG}$  and  $M_b$  relation.



No of data points	$R_{XY}$			RMSE			Slope			Intercept		
	GOR1	GOR2	SLR	GOR1	GOR2	SLR	GOR1	GOR2	SLR	GOR1	GOR2	SLR
586	0.91	0.66	0.66	0.17	0.36	0.31	$0.890 \pm 0.001$	$0.980 \pm 0.030$	$0.800 \pm 0.020$	$0.730 \pm 0.070$	$-0.200 \pm 0.230$	$1.280 \pm 0.140$
641	0.55	0.42	0.42	0.36	0.54	0.40	$1.470 \pm 0.005$	$2.660 \pm 0.130$	$1.290 \pm 0.060$	$-2.590 \pm 0.310$	$-9.580 \pm 0.760$	$-1.610 \pm 0.360$
980	0.90	0.65	0.65	0.18	0.37	0.35	$0.930 \pm 0.001$	$1.040 \pm 0.020$	$0.830 \pm 0.190$	$0.496 \pm 0.060$	$-0.160 \pm 0.190$	$1.090 \pm 0.120$
1266	0.52	0.39	0.39	0.38	0.61	0.43	$1.420 \pm 0.004$	$2.750 \pm 0.090$	$1.250 \pm 0.040$	$-2.180 \pm 0.220$	$-9.910 \pm 0.590$	$-1.160 \pm 0.250$
1385	0.89	0.71	0.71	0.18	0.34	0.32	$1.040 \pm 0.004$	$1.170 \pm 0.020$	$0.960 \pm 0.020$	$-0.160 \pm 0.060$	$-0.880 \pm 0.150$	$0.370 \pm 0.100$
1566	0.90	0.65	0.65	0.18	0.37	0.35	$0.920 \pm 0.001$	$1.020 \pm 0.020$	$0.820 \pm 0.020$	$0.584 \pm 0.050$	$-0.022 \pm 0.150$	$1.170 \pm 0.100$
6690	0.99	0.96	0.96	0.05	0.10	0.10	$1.010 \pm 0.0001$	$1.020 \pm 0.002$	$0.990 \pm 0.002$	$-0.057 \pm 0.010$	$-0.110 \pm 0.020$	$-0.010 \pm 0.010$
12896	0.98	0.94	0.94	0.09	0.17	0.17	$0.990 \pm 0.000$	$1.010 \pm 0.002$	$0.980 \pm 0.002$	$0.008 \pm 0.006$	$-0.0746 \pm 0.019$	$0.090 \pm 0.010$

Table 1. Comparison of regression parameters for GOR1, GOR2, and SLR using global datasets. Data points 586 for  $M_{S,NEIC}$  to  $M_e$ ; 614 for  $m_{b,NEIC}$  to  $M_e$ ; 980 for  $M_{s,ISC}$  to  $M_e$ ; 1266 for  $m_{b,ISC}$  to  $M_e$ ; 1385 for  $M_{wg}$  to  $M_e$ ; 1566 for  $M_s$  to  $M_e$ ; 6690 for  $M_{WG,GCMT}$  to  $M_{WG,NEIC}$ ; 12896 for  $M_{s,ISC}$  to  $M_{s,NEIC}$ .

Following the above Fuller's model, residual plots for magnitude scaling relations are shown in Figure 3. For example, of 614 ( $m_b$ ,  $M_e$ ) data pairs in Figure 2(e), 89.082% have both the positive and negative residuals, while 10.92% have only positive residuals. This scaling relation is not linear as was in other cases (Figure 3). However, in general, compared to a nonlinear relation, a linear relation will be statistically better as for error handling. As established recently, the nonlinear relation (Giacomo et al., 2015) between the  $m_b$  and  $M_w$  is not fitted well in broader ranges. Thus, the fitting of linear scaling relations amongst magnitude scales is justifiable according to Fuller's model, Figure 3.

## 5. SUMMARY AND CONCLUSIONS

We have developed scaling relations between different magnitudes (e.g.,  $m_b$  and  $M_s$ ) and a preferred magnitude ( $M_e$ ), using SLR, GOR1, and GOR2 techniques. Because it reduces GOR2 bias, the GOR1 is the best regression procedure for converting different seismic magnitudes into a preferred magnitude - as previous studies, e.g., Das et al. (2018), had already suggested. Earthquake catalogs generally contain different magnitude scales, where  $M_w$  and  $M_e$  are the scales commonly used in seismic literature for denoting earthquake size. However, a homogenized earthquake catalog using scaling relations represents the most critical need for seismicity and seismic hazard assessment studies.

Unified catalogs in terms of  $M_w$  are already available in the literature. Recent studies, e.g., by Bormann and Saul (2009) and Das et al. (2019), suggest that  $M_w$  is not appropriate for representing the earthquake size over the entire globe because that scale was developed mainly for Southern California and is unvalidated in a global context for weaker and intermediate earthquakes. Furthermore, the  $M_w$  scale systematically underestimates the strongest earthquakes (Bormann and Saul, 2009, Stein and Okal, 2005, Das et al., 2019) and overestimates the weakest and intermediate earthquakes. Furthermore, many studies, e.g., by Giacomo et al. (2010) and Das et al. (2019), have suggested that the  $M_w$  does not correlate well with the high-frequency ground motion that is of importance for engineering

applications. An updated physics-based scale, the  $M_{wg}$ , was developed in a recent study by Das et al. (2019). It reduces the underestimation and overestimation problem of the  $M_w$  scale. Also, the  $M_{wg}$  provides a better correlation with high- and low-frequency ground motion. Another scale, the  $M_e$ , represents earthquake size in terms of the seismic energy radiated by an earthquake, although the  $M_e$  is not sufficiently available in seismic catalogs due to the complexity of its determination and the associated great uncertainty. However, the  $M_e$  is a scale very useful in understanding seismicity in terms of energy radiation. Borman and Giacomo (2010) emphasized the use of  $M_w$  and  $M_e$  together for seismic hazard assessments because the  $M_w$  scale alone is insufficient for representing damage potential. Bormann et al. (2002) found that it takes more than one magnitude to describe essential differences in the source process.

Direct  $M_e$  estimations from velocity broadband records have become a routine at the United States Geological Survey (USGS) National Earthquake Information Center (NEIC) since 1987, whereas seismic moment has been measured and cataloged since 1976. Although direct observed  $M_e$  values are still not sufficiently available, the scaling relations here developed from different magnitudes can be used to obtain proxy  $M_e$  values.

In that respect, global scaling relations between the  $m_b$ ,  $M_s$ ,  $M_{wg}$ , and  $M_e$  scales were developed based on GOR1, GOR2, and SLR statistical methods. The background of different statistical methods (GOR1 and GOR2) adopted for scaling relations also has been provided. As to comparisons, this study has found that, for the here examined datasets, GOR1-derived magnitude relations are better than GOR2- and SLR-derived magnitude relations, Table 1. Also, GOR1 and SLR slopes are closer when compared to GOR2, Table 1. Furthermore, there is no substantial difference between the results for SLR and GOR1; however, a considerably big difference exists between the SLR- and GOR2-derived magnitude relations due to the incorrect use of GOR2 as reported in earlier studies, e.g., by Stefanski (2000), Carroll and Rupert (1996), and Das et al. (2018). While in some cases, the mean values in the estimates of GOR1 and SLR do not exhibit any substantial difference, there would be a significant difference between SLR and GOR1 on consideration of errors.

To derive the relations, we compiled  $M_s$  magnitude data for 13,576 events from ISC and 13,282 events from NEIC, the  $m_b$  magnitude data for 1,266 events from ISC and 614 events from NEIC, and the  $M_{wg}$  magnitude values for 6,690 events from NEIC and GCMT.

We have derived the  $M_{S,ISC}$ -to- $M_e$  and  $M_{S,NEIC}$ -to- $M_e$  conversion relations for magnitude ranges of  $4.7 \leq M_{S,ISC} \leq 8.0$  and  $4.5 \leq M_{S,NEIC} \leq 8.0$ , respectively. Eqns. (13) & (14) show that the  $M_{S,ISC}$  and  $M_{S,NEIC}$  are nearly equivalent, as found in other studies, e.g., by Das et al. (2011), Utsu (2002), and Das and Wason (2010). This equivalence allows considering  $M_s$  for conversion into  $M_e$  by ISC and NEIC as a homogenous dataset. Furthermore, we have derived the  $m_{b,ISC}$ -to- $M_e$  and  $m_{b,NEIC}$ -to- $M_e$  conversion relations for magnitude ranges of  $5.2 \leq m_{b,ISC} \leq 6.2$  and  $5.3 \leq m_{b,NEIC} \leq 6.5$ . Finally, we have derived the  $M_{wg}$ -to- $M_e$  conversion relation for magnitude ranges of  $5.2 \leq M_{wg} \leq 8.2$  with focal depths  $< 70$  km.

As derived from global data, the here obtained regression relations enable a better understanding of seismicity. As such, they are of use in geophysical investigations, including crustal deformation studies. Other applications include developing homogenous earthquake catalogs for specific seismic regions in the absence of regional regression relations for magnitude conversions. We recommend seismological data centers start distributing the  $M_e$  to foster a better understanding of seismicity and seismic hazard.

#### ACKNOWLEDGMENTS

This research was supported by the FONDECYT (grant No. 11200618), CORFO (grant ING203016EN12), and CONICYT/FONDAP (grant 15100017). The authors are grateful to three anonymous reviewers for critical reviews and constructive suggestions, which significantly helped improve this paper.

#### REFERENCES

Adcock, R.J. (1878) A problem in least squares. *The Analyst* 5:53–54

Beresnev, I.A. (2009) The reality of the scaling law of earthquake-source spectra. *J. Seism.* 13:433-436

Boatwright, J., Choy, G.L. (1986) Teleseismic estimates of the energy radiated by shallow earthquakes. *J. Geophys. Res.* 91:2095–2112

Bormann, P., Baumbach, M., Bock, M., Gresser, H., Choy, G.L., Boatwright, J. (2002) *Seismic sources and source parameters*. In: Bormann, P. (Ed.), in: IASPEI New Manual Seismological Observatory Practice, GeoForschungsZentrum Potsdam, Vol. 1, Chapter 3, 94 pp.

Bormann P, Liu, R., Xu., Z., Ren, K., Zhang, L., Wendt, S (2009) First application of the new IASPEI teleseismic magnitude standards to data of the China National Seismographic Network. *Bull. Seism. Soc. Am.* 99(3):1868-1891

Bormann, P., Saul, J. (2009) *Earthquake Magnitude*. Ency. Complex. Appl. Syst. Sci., 3, pp. 2473–2496

Bormann, P., Giacomo, D.D. (2010) The moment magnitude  $M_w$  and the energy magnitude  $M_e$ : Common roots and differences, *J. Seismol.* 15:411–427

Bormann, P. (2020) *Earthquake Magnitude*. Encyclopedia of Solid Earth Geophysics, Encycl. Ea. Sci. Ser.

Carroll, R.J., Ruppert, D. (1996) The use and misuse of orthogonal regression estimation in linear errors-in-variables models. *The Amer. Statist.* 50(1):1–6

Choy, G.L., Boatwright, J. (1995) Global patterns of radiated seismic energy and apparent stress. *J. Geophys. Res.* 100:18205–18228

Choy, G.L., Kirby, S. (2004) Apparent stress, fault maturity and seismic hazard for normal-fault earthquakes at subduction zones. *Geophys. J. Int.* 159:991–1012

Castellaro, S., Mulargia, F., Kagan, Y.Y. (2006) Regression problems for magnitudes. *Geophys. J. Int.* 165:913-930

Das, R., Wason, H.R. (2010) Comment on "A homogenous and complete earthquake catalog for Northeast India and the adjoining region" by Yadav, R.B.S., Bormann, P., Rastogi, B.K., Das, M.C., Chopra, S., *Seism. Res. Lett.* 81(2):232-234

Das, R., Wason, H.R., Sharma, M.L. (2011) Global regression relations for conversion of surface wave and body wave magnitudes to moment magnitude. *Natu. Haza.* 59(2):801-810

Das, R., Wason, H.R., Sharma, M.L. (2012) Magnitude conversion to unified moment magnitude using orthogonal regression. *Jour. Asi. Ear. Sci.* 50(2):44-51

Das, R., Wason, H.R., Sharma, M.L. (2013) General Orthogonal Regression Relations between body wave and moment magnitudes, *Seismol. Res. Lett.* 84:219-224

Das, R., Wason, H.R., Sharma, M.L. (2014) Unbiased Estimation of Moment Magnitude from Body and Surface Wave Magnitude. *Bull. Seism. Soc. Am.* 104(4):1802-1811

Das, R., Wason, H.R., Gonzalez, G., Sharma, M.L., Choudhury, D., Narayan., R., Pablo, S. (2018) Earthquake Magnitude Conversion Problem. *Bull. Seism. Soc. Am.* 108(4):1995-2007

Das, R., Sharma, M.L., Wason, H.R., Choudhury, D., Gonzalez, G. (2019) A seismic moment magnitude scale. *Bull. Seism. Soc. Am.* 109(4):1542-1555

Fuller, W.A. (1987) *Measurement Error Models*. Wiley, New York, USA.

Giacomo, D, Parolai, D.S., Bormann, P., Gresser, H., Saul, J., Wang, R., Zschau, J. (2010) Suitability of rapid energy magnitude estimations for emergency response purposes. *Geophys. J. Int.* 180:361-374

Giacomo, D. (2011) Determination of the energy magnitude  $M_E$ : application to rapid response purposes and insights to regional/local variabilities. University of Potsdam, Germany

Giacomo, D., Bondár, D.I., Storchak, D.A., Engdahl, E.R., Bormann, P., Harris, J. (2015) ISC-GEM: Global Instrumental Earthquake Catalogue (1900–2009): III. Recomputed  $M_s$  and  $m_b$ , proxy  $M_w$ , final magnitude composition and completeness assessment. *Phys. Earth Planet. In.* 239:33–47

Gutenberg, B. (1945a) Amplitude of surface waves and magnitude of shallow earthquakes. *Bull. Seism. Soc. Am.* 35:3–12

Gutenberg, B. (1945b) Amplitudes of P, PP and S and magnitudes of shallow earthquakes. *Bull. Seism. Soc. Am.* 35:57-69

Gutenberg, B., Richter, C.F. (1956) Earthquake magnitude, intensity, energy, and acceleration (second paper). *Bull. Seism. Soc. Am.* 46(2):105–145

Hanks, T.C., Kanamori, H. (1979) A moment magnitude scale. *J. Geophys. Res.* 84:2348-2350

IASPEI (2013) Summary of Magnitude Working Group Recomms. on Standard Procedures for Determining Earthquake Magnitudes from Digital Data; [www.iaspei.org/commissions/CSOI/Summary\\_of\\_WG\\_recommendations.pdf](http://www.iaspei.org/commissions/CSOI/Summary_of_WG_recommendations.pdf)

Kanamori, H. (1977) The energy release in great earthquakes. *J. Geophys. Res.* 82:2981-2987

Kendall, M.G., Stuart, A. (1979) *The Advanced Theory of Statistics*. Vol. 24th ed. Griffin, London, United Kingdom

- Kummel, C.H. (1879) Reduction of Observed Equations Which Contain More Than One Observed Quantity. *The Analyst* 6:97-105
- Lindley (1947) Regression lines and the linear functional relation. *J. Roy. Statist. Soc. Suppl.* 9:218-244
- Madansky, A. (1959) The fitting of straight lines when both variables are subject to error. *The Amer. Statist.* 54(285):173-205
- Nath, S.K., Thingbaijam, K.K.S. (2010) Comment on "Estimation of seismicity parameters for India". *Seism. Res. Lett.* 81:1001-1003
- Petrova, N.V., Gabsatarova, P.I. (2019) Depth corrections to surface-wave magnitudes for intermediate and deep earthquakes in the regions of North Eurasia. *J. Seismo.* 24:203-219
- Press, W.H., Teukolsky, S.A., Vetterling, W.T. (1992) *Numerical Recipes in C: The Art of Scientific Computing*. Cambridge University Press, United Kingdom
- Pearson, K. (1901) On Lines and Planes of Closest Fit to systems of Points in Space. *Philos. Mag.* 2:559-572
- Richter, C.F. (1935) An instrumental earthquake magnitude scale. *Bull. Seism. Soc. Am.* 25(1):1-32
- Ristau, J. (2009) Comparison of magnitude estimates for New Zealand earthquakes: moment magnitude, local magnitude, and teleseismic body-wave magnitude. *Bull. Seism. Soc. Am.* 99(3):1841-1852
- Scordilis, E.M. (2006) Empirical global relations converting  $M_s$  and  $m_b$  to moment magnitude. *J. Seism.* 10:225-236
- Stefanski, L.A. (2000) Measurement Error Models. *Amer. Statist. Assoc.* 95:452:1353-1358
- Stein, S., Okal, E. (2005) Speed and size of the Sumatra earthquake. *Nature* 434:581-582
- Stromeier, D., Grünthal, G., Wahlström, R. (2004) Chi-square regression for seismic strength parameter relations, and their uncertainties, with application to an  $M_w$  based earthquake catalogue for central, northern and northwestern Europe. *J. Seism.* 8:143-153
- Thingbaijam, K.K.S., Nath, S.K., Yadav, A., Raj, A., Walling, M.Y., Mohanty, W.K. (2008) Recent seismicity in Northeast India and its adjoining region. *J. Seism.* 12:107-123
- Utsu, T. (2002) Relations between magnitude scales. In: *International Handbook of Earthquake and Engineering Seismology*, Part A, W. H. K. Lee, H. Kanamori, P. C. Jennings and C. Kisslinger (Eds.). Academic Press, Amsterdam, the Netherlands, 81(A):733-746
- Vanek, J., Zatopek, A., Karnik, V., Kondorskaya, N.V., Riznichenko, Y.V., Savarensky, E.F., Soloviev, S.L., Shebalin, N.V. (1962) Standardization of magnitude scales. *Bull. Acad. Sci. USSR Geophys Ser.* 108-111
- Wason, H.R., Das, R., Sharma, M.L. (2012) Magnitude conversion problem using general orthogonal regression. *Geophys. J. Int.* 190(2):1091-1096
- Yadav, R.B.S., Bormann, P., Rastogi, B.K., Das, M.C., Chopra, S. (2009) A homogeneous and complete earthquake catalog for northeast India and the adjoining region. *Seismol. Res. Lett.* 80(4):609-627.
-